THE JOURNAL OF PHYSICAL CHEMISTRY B

Article

pubs.acs.org/JPCB

Probing the Solvent Accessibility of the [4Fe−4S] Cluster of the Hydrogenase Maturation Protein HydF from *Thermotoga neapolitana* by HYSCORE and 3p-ESEEM

Marco Albertini,[†] Paola Berto,[‡] Francesca Vallese,[‡] Marilena Di Valentin,[†] Paola Costantini,*[,§] and Donatella Carbonera*[,†]

[†]Department of Chemical Sciences, University of Padova, Via F. Marzolo 1, 35131 Padova, Italy

[‡]Department of Biomedical Sciences, University of Padova, Viale G. Colombo 3, 35131 Padova, Italy

[§]Department of Biology, University of Padova, Viale G. Colombo 3, 35131 Padova, Italy

Supporting Information

ABSTRACT: The catalytic site of [FeFe]-hydrogenase, the "H-cluster", composed of a [4Fe−4S] unit connected by a cysteinyl residue to a [2Fe] center coordinated by three CO, two CN^-, and a bridging dithiolate, is assembled in a complex maturation pathway, at present not fully characterized, involving three conserved proteins, HydG, HydE, and HydF. HydF is a complex enzyme, which is thought to act as a scaffold and carrier for the [2Fe] subunit of the H-cluster. This maturase protein contains itself a [4Fe−4S] cluster binding site, with three conserved cysteine residues and a noncysteinyl fourth ligand. In this work, we have exploited 3p-ESEEM and HYSCORE spectroscopies to get insight into the structure and the chemical environment of the [4Fe−4S] cluster of HydF from the hyperthermophilic organism *Thermotoga neapolitana*. The nature of the fourth ligand and the solvent accessibility of the active site comprising the [4Fe−4S] cluster are discussed on the basis of the spectroscopic results obtained upon H/D exchange. We propose that the noncysteinyl ligated Fe atom of the [4Fe−4S] cluster is the site where the [2Fe] subcluster precursor is anchored and finally processed to be delivered to the hydrogenase (HydA).

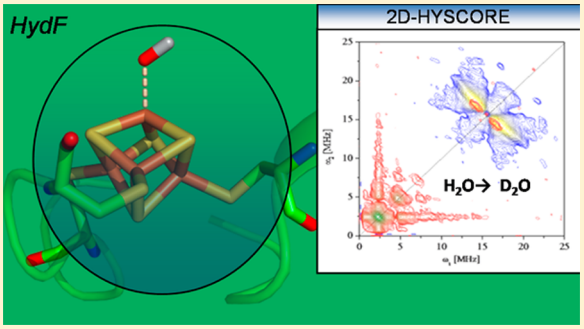

INTRODUCTION

Iron−sulfur (FeS) clusters are pivotal cofactors of several enzymes involved in major biochemical processes in prokaryotic and eukaryotic organisms.[1] FeS proteins are among the most important electron carriers, spanning a wide range of reduction potentials (from −700 to +400 mV). As a consequence, they play important roles in the mitochondrial respiratory chain as well as in photosynthesis. These clusters are also involved in coupling of electron and proton transfer, substrate binding and activation and are essential in determining protein structure, regulation of gene expression and enzymatic activity, disulfide reduction and iron, electron, or cluster storage.[2,3] Composed of iron and inorganic sulfur, they are most frequently found in a cubane form that contains four Fe and four S atoms (i.e., [4Fe−4S]), although simpler arrangements, of two Fe and two S units (i.e., [2Fe−2S]), or more complex clusters, as in hydrogenase proteins,[3,4] also exist.

The hydrogenases are a class of enzymes that have been subjected to extensive studies aimed at their exploitation for biotechnological renewable energy production due to the capability to reversibly reduce protons to hydrogen gas, according to the reaction $2H^+ + 2e^- \leftrightarrow H_2$.[5] This conceptually simple reaction occurs at an unusually complex metal cluster, the so-called H-cluster, composed of a [2Fe] center ligated to a [4Fe−4S] cubane by a cysteine thiolate,[6] with the two iron atoms coordinated by carbon monoxide and cyanide, and by a dithiomethylammine molecule as a bridge.[6−8] The assembly of this composite active site follows biosynthetic rules common to other phylogenetically unrelated FeS cluster systems and can be split in two main steps: (i) the synthesis of a cluster precursor on a scaffold protein and (ii) the transfer of this precursor to the target apoprotein, which is eventually converted to the active form. Although the overall process of [4Fe−4S] and [2Fe−2S] cluster biogenesis has been thoroughly investigated and described in detail in bacteria as well as in eukaryotic intracellular compartments (reviewed in ref 2), the assembly of the [FeFe]-hydrogenases H-cluster, which is complicated by the presence of nonprotein ligands, is at present not fully understood. As for other FeS proteins, this process involves the participation of several enzymes and cofactors, including three conserved maturation proteins, that is, HydE and HydG, two radical *S*-adenosylmethionine (SAM) enzymes, and HydF, a

Special Issue: Wolfgang Lubitz Festschrift

Received: March 31, 2015
Revised: May 15, 2015
Published: May 15, 2015

DOI: 10.1021/acs.jpcb.5b03110
J. Phys. Chem. B 2015, 119, 13680−13689

GTPase containing an FeS cluster binding motif.[9] Important advances made in recent years have provided a deeper understanding of the overall complexity of this pathway, and a model has been proposed (reviewed in ref 10) in which the role of the entire HydE/HydF/HydG maturation machinery is to synthesize and insert a [2Fe] subcluster, together with its ligands, into a hydrogenase containing a preformed [4Fe−4S] unit.[11] In this model, the maturase HydF works as a scaffold to accommodate HydE and HydG for the chemical modification of the H-cluster precursor[12−17] and as a carrier, in a second step, to deliver the cluster to HydA, thus completing the maturation process. Interestingly, it has been shown that H-cluster synthetic mimics can be loaded on a recombinant HydF protein and then transferred to an apohydrogenase,[18,19] thus providing additional mechanistic evidence of the [FeFe]-hydrogenases maturation process stepwise nature. More recently, Kuchenreuther et al. have shown that HydG is the site where a $Fe(CO)_2(CN)$ synthon is initially formed as an integral part of a pre-existing [4Fe−4S] framework, giving rise to a $Fe_3S_4Fe(CO)_2(CN)$ cluster.[20,21] In their work the authors suggest that two of these complex synthons may assemble together with a dithiolate bridge to form the [2Fe] subcluster. However, the mechanism allowing the final assembly of the two synthons and the transfer of these moieties to apo-HydA (which contains the [4Fe−4S] component of the H-cluster but not the [2Fe] subsite) remains unclear. Also unknown is the specific role of HydE and HydF, although it has been shown that these proteins have a key function in the maturation process because *C. reinhardtii* recombinant mutant strains, lacking single or combinations of maturases, are completely unable to express an active [FeFe]-hydrogenase.[9,22] FTIR, EPR, and EXAFS experiments on HydF from *C. acetobutylicum*, which has been expressed in its native background with HydE and HydG, demonstrate that a binuclear iron species similar to the H-cluster is present in fully assembled HydF.[23,24] Recent work on HydE has indicated that the product of HydE catalysis could link together two of the $Fe(CO)_2CN$ units to accomplish [2Fe] subcluster formation on HydF.[25] Moreover, the high binding affinity between HydE and HydF,[17] together with the existence of a hydEF fusion gene in some organisms,[9] indicates that HydE and HydF work in synergy. Thus, it may be possible that a binuclear [2Fe] cofactor presynthesized by HydG and bridged by HydE is introduced, at some stage of its maturation, into HydF. According to this hypothesis, the [4Fe−4S] cluster of HydF could anchor the 2Fe precursor during the final assembly before the transfer to HydA. In this context, a detailed spectroscopic characterization of the [4Fe−4S] cluster of HydF represents an important step to get insight into the chemistry taking place at that site.

All HydF proteins identified to date share an FeS cluster binding motif ($CxHx_{46-53}HCxxC$) in their C-terminal end,[26] with three highly conserved cysteine residues that bind the [4Fe−4S] cluster. We solved the three-dimensional crystal structure of the HydF apoprotein (i.e., lacking both the GTP substrate and the [4Fe−4S] cluster) from the hyperthermophilic bacterium *T. neapolitana* (PDB ID: 3QQ5)[27] and described the domain containing the consensus sequence, highly conserved, for the binding of a [4Fe−4S] cluster (i.e., $CxHx_{46-53}HCxxC$). We explored the [4Fe−4S] cluster coordination sphere of HydF recombinant proteins from *T. neapolitana* ($HydF_{T.n.}$) and from *C. acetobutylicum* ($HydF_{C.a.}$) by combining a site-specific mutagenesis approach, based on the 3D model structure and on a sequence alignment, with continuous-wave electron paramagnetic resonance (CW-EPR) and hyperfine sublevel correlation (HYSCORE) spectroscopies.[28] We found that the three conserved cysteines from the $CxHx_{46-53}HCxxC$ sequence are strictly required for cluster coordination in the HydF from both species, whereas a definite, but dispensable, nitrogen-based ligation, assigned to a histidine, was found only for the cluster of HydF from *C. acetobutylicum*. Instead, a nitrogen-based ligand was excluded for *T. neapolitana*.[28] The diversity between the two species is surprising because the two histidine residues in the consensus sequence are conserved and there is an expected large structural similarity of the cluster binding pockets.[27] However, it is worth noting that, as Berggren et al. suggested,[29] the Strep-tag II (an eight amino acid oligopeptide featuring a histidine residue) used in the purification of HydF from *C. acetobutylicum* could give an adventitious histidinyl ligation. Thus, at present, it cannot be excluded that also the [4Fe−4S] cluster of the wild-type HydF from *C. acetobutylicum* presents, in its native form, a nonhistidinyl fourth ligand. In any case, the results obtained in the different organisms have indicated that while the three cysteines of the cluster binding consensus sequence are all essential for the assembly of a functional [4Fe−4S] center, the two histidines of the conserved sequence are not decisive for metal coordination, even in *C. acetobutylicum*, because after removal, they result in being replaced by other ligands.[28] Although cysteine and histidine are ubiquitous iron ligands, alternative ligands such as aspartate, serine, arginine, or glutamine have been reported for several Fe−S proteins.[3,30,31] Noncysteinyl ligation to a cubane-type FeS cluster is known to occur in several enzymes, and in each case, the atypical cluster coordination has a functional significance.[32] The ligand to the fourth iron may also be a small molecule from the buffer.[33] The unusual coordination to the fourth iron makes it labile, explaining why in many cases proteins of this kind are found to contain $[3Fe-4S]^+$ clusters in their as-isolated or air-exposed states, as was also observed for HydF.[28] Upon reduction with a reducing agent, such as dithionite or photoreduced 5-deazariboflavin, the $[3Fe-4S]^+$ clusters can usually be reconverted to the $[4Fe-4S]^+$ clusters by scavenging of adventitious iron or by cannibalization of a fraction of the clusters.[34] Protein-bound $[3Fe-4S]^+$ clusters are generally derived from $[Fe_4S_4(S\text{-}Cys)_3L]$ centers with $L = H_2O/OH^-$, a side-chain carboxylate, or some other noncysteinate ligand.[35] It has been suggested that, under oxidizing conditions, the reaction $[Fe_4S_4]^{3+} \rightarrow [Fe_3S_4]^+ + Fe^{2+}$ may occur, with the removal of the ferrous ion being assisted by the complexation with an exogenous ligand.[36]

In our previous work, we analyzed the low-temperature CW-EPR spectra of a series of site-directed mutants (D310A, D337A, E300A, and Y380A), corresponding to residues that are in close proximity to the [4Fe−4S] cluster binding site, according to the crystal structure of apo-$HydF_{T.n.}$,[37] in order to investigate this crucial problem of the cluster ligation. These residues were considered putative cluster ligands. HYSCORE spectra of the mutants were acquired and compared to those of the wild-type protein.[37] The results showed however that the [4Fe−4S] cluster was only slightly affected by the substitution of D310A, D337A, E300A, and Y380A with alanine, meaning that the assembly of the cluster was not compromised or altered by the removal of these residues. Thus, it seems likely that either the selected residues are not directly involved in the ligation of the [4Fe−4S] cluster or they can be easily substituted by other residues. Interestingly, the HYSCORE

DOI: 10.1021/acs.jpcb.5b03110
J. Phys. Chem. B 2015, 119, 13680−13689

spectrum of wild-type $HydF_{T.n.}$ revealed the presence of peaks due to the interaction of the metal center with surroundings protons.[28] In this work, we combine HYSCORE and electron spin−echo envelope modulation (ESEEM) spectroscopies with H_2O/D_2O exchange to explore the exchangeability of these protons, to evaluate the accessibility of the water solvent molecules into the protein cavity harboring the cluster, and to investigate the nature of the fourth ligand of the cluster.

MATERIALS AND METHODS

Heterologous Expression and Purification of HydF Protein from *T. neapolitana*. The *hydF* gene ($hydF_{T.n.}$) was isolated from purified genomic DNA by PCR amplification and subcloned in frame with a 6His-tag sequence at the N-terminus in a pET-15b vector (from Novagen).[28,37] Site-directed mutagenesis of the *hydF* gene at selected sites was performed with the QuickChange II Site-Directed Mutagenesis Kit (from Stratagene), using as template $pET\text{-}15b/hydF_{T.n.}$ recombinant plasmid. *Escherichia coli* Rosetta (DE3) cells were transformed with the obtained $pET\text{-}15b/hydF_{T.n.}$ plasmids, and positive clones were selected by antibiotic resistance. The wild-type and mutant 6His-tagged $HydF_{T.n.}$ proteins were expressed in anaerobic conditions, using 1−2 L cultures, and purified by affinity chromatography and gel filtration. Briefly, cells were harvested by centrifugation, resuspended in lysis buffer (25 mM Tris-HCl pH 8, 200 mM KCl, and protease inhibitors 1 μg/mL pepstatin A, 1 μg/mL leupeptin, 1 μg/mL antipain, 1 mM PMSF) and lysed by a French press. The supernatant fractions were isolated from cell debris by centrifugation and the proteins purified to homogeneity by combining a nickel affinity chromatography (HIS-Select Nickel Affinity Gel, from Sigma-Aldrich) and gel filtration chromatography using a Superose 12 10/300 GL column (from GE Healthcare), equilibrated in lysis buffer. The proteins were finally concentrated. Samples for H/D exchange analysis were obtained by reiterated dilution and concentration in D_2O and 200 mM NaCl to a final concentration of 600 μM. All purification steps were performed under anaerobic conditions in a glovebox with O_2-free solutions.[27]

EPR Spectroscopy. EPR tubes of untreated and D_2O-exchanged $HydF_{T.n.}$ were filled in an anaerobic box and frozen in liquid nitrogen. Reduction of the HydF samples was achieved by supplementing the proteins with 20 mM sodium dithionite, by adding a few microliters of a concentrated solution in an anaerobic buffer and incubating for 10 min before freezing. All samples were stored in liquid nitrogen until spectral acquisition. Low-temperature CW-EPR spectra were recorded using a Bruker Elexsys E580-X-band spectrometer equipped with a ER4102ST cavity and a helium flow cryostat (ESR 900 Oxford Instruments). Acquisition parameters were the following: temperature = 10 K; microwave frequency = 9.38 GHz; modulation frequency = 100 kHz; modulation amplitude = 1.0 mT; microwave power = 2.0 mW; time constant = 163.84 ms; conversion time = 81.92 ms; number of data points = 4096 (scan range = 700 mT). Simulations of the CW-EPR spectra were performed using the *pepper* routine of the *Easyspin* package in Matlab;[38] g values were estimated by calibration with a strong-pitch sample.

Pulsed EPR Measurements and Data Processing. Pulsed EPR experiments were carried out using the same spectrometer equipped with a dielectric ring resonator (ER4118X-MD5) and a helium flow cryostat (Oxford CF935) at a temperature of 10 K. The three-pulse ESEEM (3p-ESEEM) measurements were performed, at several different values of the external magnetic field, applying a stimulated echo sequence $[(\pi/2)-\tau-(\pi/2)-T-(\pi/2)-\tau-\text{echo})$ with a τ value ranging from 192 to 256 ns to account for the dependence of the blind spots upon the external magnetic field and for both suppression of the free Larmor proton frequency and enhancement of the deuterium modulation. A 16 ns detector gate centered at the maximum of the echo signal was applied. The length of the $\pi/2$ pulse was set to 16 ns. The echo intensity was monitored as a function of T, incremented in steps of 8 ns from the initial value of 20 ns. A total of 512 points were collected at a 1200 Hz repetition rate. A four-step phase cycle was applied to remove unwanted echoes. The final 10 points of the time trace were acquired with the integration window positioned 400 ns off of the echo to define the background. The ESEEM data were processed for analysis both in the time and in the frequency domain with a home-written program in MATLAB following the ratio method introduced by Mims et al.[39] The envelope obtained for the D_2O-exchanged sample was divided by the envelope obtained for the untreated sample, after normalization of both envelopes. The quotient time trace was dead-time reconstructed according to the procedure described by Mims.[40] The trace was then apodized with a Hamming window function, zero-filled to 2048 data points, and subjected to cosine Fourier transformation to obtain the frequency domain spectra.

The HYSCORE measurements were performed by applying a conventional two-dimensional (2D) four-pulse sequence $[(\pi/2)-\tau-(\pi/2)-t_1-(\pi)-t_2-(\pi/2)-\tau-\text{echo})$ with a τ delay ranging from 192 to 256 ns for the untreated and D_2O-exchanged sample to compensate for blind spots and for both suppression of the free Larmor proton modulation and enhancement of the deuterium modulation. An 8 ns detector gate was applied, centered at the maximum of the echo signal. The nominal duration of both the $\pi/2$ and π pulses was 16 ns. The echo intensity was measured as a function of t_1 and t_2, incremented in steps of 8 or 12 ns from the initial value of 20 ns. HYSCORE data were collected in the form of 2D time domain patterns as a 256 × 256 matrix at a repetition rate of 1200 Hz. A four-step phase cycling procedure was used to remove unwanted echoes. Spectral processing was performed using a home-written MATLAB routine. The 2D time domain data were corrected for the relaxation decay by a third-order polynomial background in both dimensions. Traces were apodized using a Hamming window function, zero-filled to 1024 points and Fourier transformed in both dimensions. The frequency map was symmetrized before plotting as a contour plot in logarithmic scale of intensity.

Simulation of ESEEM and HYSCORE Data. Simulation of both the time and frequency domain of 3p-ESEEM data was performed with a home-written FORTRAN routine that computes the modulation of the time domain due to the single-electron spin manifolds, V^{α} and V^{β}, for any active nucleus considered. The modulations were then combined according to the exact product rule for 3p-ESEEM with a home-written MATLAB program to obtain the full modulation pattern. Frequency domain spectra were obtained by cosine Fourier transformation of the time traces. The input parameters for the simulation were the external magnetic field value, the number of the nuclei, the isotropic hyperfine coupling parameter a_{iso}, the principal values of the dipolar hyperfine tensor (assumed to be axial $[T, T, -2T]$ for simplicity due to the lack of structural information and on the basis of the relatively long distance of

DOI: 10.1021/acs.jpcb.5b03110
J. Phys. Chem. B 2015, 119, 13680−13689

weakly interacting protons from the spin-carrying center), and the quadrupolar interaction parameters e^2qQ and η. Spherical averaging of the interaction tensors was applied. Hyperfine parameters were chosen to obtain the best simulation, while the quadrupolar parameters were slightly adjusted (e^2qQ = 0.20 MHz and η = 0) starting from the reported data for Ice II.[41]

Simulation of HYSCORE spectra was performed on the frequency domain using a home-written MATLAB program based on the *saffron* routine of the *Easyspin* package.[42] The spherical averaging limit of the interaction tensors, as implemented in the *Easyspin* package, was adopted in the calculation. The same input parameters described previously for the 3p-ESEEM were applied. The calculated 2D spectra are presented as a contour plot in logarithmic scale of intensity. The spherical averaging adopted in both the 3p-ESEEM and HYSCORE simulations was justified by the scarce dependence of the spectral shape on the magnetic field observed in the experimental data, as discussed in the Results and Discussion sections.

RESULTS

In order to characterize the proton environment of the [4Fe−4S] cluster of $HydF_{T.n.}$ and possibly assign the fourth ligand to a protonated species, proton/deuteron (H/D) exchange experiments were performed combined with CW-EPR, three-pulse ESEEM, and HYSCORE spectroscopies.

It is known that $[4Fe{-}4S]^{2+}$ clusters give rise to EPR signals after chemical reduction to $[4Fe{-}4S]^{+}$ (usually an S = 1/2 state). The low-temperature CW-EPR spectra of chemically reduced $HydF_{T.n.}$, detected before and after the H/D exchange, are compared in Figure 1. The spectrum after the treatment

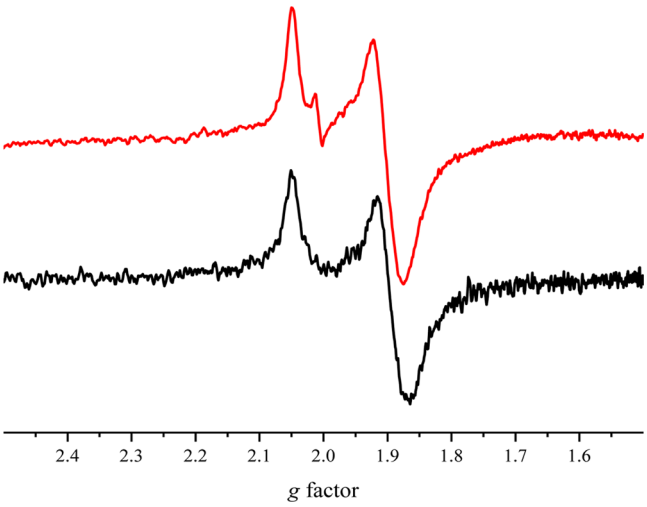

Figure 1. X-band CW-EPR spectra of chemically reduced HydF from *Thermotoga neapolitana* detected before (red) and after H/D exchange (black). T = 10 K. Spectrometer parameters are reported in the Materials and Methods section.

remains substantially unchanged except for a very small shift of the X principal value of the g tensor toward lower values and a minor increment of the g strain along the same direction (Table 1), proving that the exchange procedure adopted does not introduce significant changes of the cluster structure. The weak narrow signal (1.6 mT), located in the g ≈ 2.003 region, clearly visible in the spectrum of $HydF_{T.n.}$ without H/D exchange, has been assigned before to a radical species, which is occasionally

Table 1. g-Tensor Principal Values and g-Strain Values As Obtained from Computer Simulation of Experimental CW-EPR Spectra of $HydF_{T.n.}$ before and after H/D Exchange

medium	[g_z g_y g_x]	line width (mT)	g strain
H_2O	[2.044 1.90 1.861]	2.5	[0.011 0.027 0.035]
D_2O	[2.052 1.90 1.859]	2.5	[0.015 0.025 0.038]

produced after reduction with sodium dithionite of wild-type and mutants HydF.[28]

HYSCORE and ESEEM spectroscopies allow measuring the weak magnetic interactions between the FeS cluster and the nearby deuterium/proton nuclei. The spectra were collected at the three different magnetic field positions corresponding to the principal values of the g tensor. As previously described, the HYSCORE map of $HydF_{T.n.}$ reveals three distinct proton ridges around 15 MHz, characterized by a very small anisotropy.[37] In Figure 2, the HYSCORE spectra of $HydF_{T.n.}$, taken before and after the H/D exchange, are reported. The spectra show significant differences in terms of the number and position of the ridges. Ridge III is the only one appearing entirely conserved upon H/D exchange (the effect is particularly evident in correspondence of the g_z position), thus supporting our previous assignment[37] to the nonexchangeable, β-cysteinyl protons of the cysteines coordinating the cluster.[43−49] On the contrary, the H/D exchange affects the sharp ridge II, which is no longer observable in the proton region of the HYSCORE spectra, suggesting an easy exchangeability of these protons. The third set of protons (ridge I) is also largely affected by the H/D exchange, although a weak signal in the proton region, clearly visible only in correspondence of the most intense spectrum detected at the g_y position, is still present. This residual ridge has a different shape with respect to the main ridge I, which has been removed by the H/D exchange, suggesting that it belongs to a fourth family of protons not observed before because of the large overlap with ridge I. The position near the diagonal line and the tiny curvature of the ridge show that the protons giving rise to this signal are characterized by a very small hyperfine interaction and can be tentatively assigned to distant, weakly coupled protons belonging to the protein environment of the cluster.

Focusing on the low-frequencies region of the HYSCORE spectra (about 2 MHz), it can be seen that several new cross peaks appear after the H/D exchange, proving that some deuterium atoms effectively approach the [4Fe−4S] cluster.

In order to disentangle the signals of this spectral region, a computer simulation of the HYSCORE spectra, before and after the H/D exchange, has been performed in correspondence of the three different values of the external magnetic field investigated. As a starting point for the simulations, we adopted the same values of the hyperfine couplings previously obtained by a graphical analysis of the spectra,[37] following a method previously described.[50] Simulation of the HYSCORE spectra of the exchangeable protons (ridges I and II) is shown in Figure 3, and corresponding parameters are reported in Table 2 for the two most significant field positions (g_y and g_z). As appearing already by a qualitative inspection of the spectra detected at different field positions, very little orientation selection is present in determining the HYSCORE maps. Indeed, a satisfying agreement with the experimental data is obtained when two different sets of protons are considered in the simulation in the spherical averaging approximation. Axial tensors for the hyperfine interaction of all estimated proton

DOI: 10.1021/acs.jpcb.5b03110
J. Phys. Chem. B 2015, 119, 13680−13689

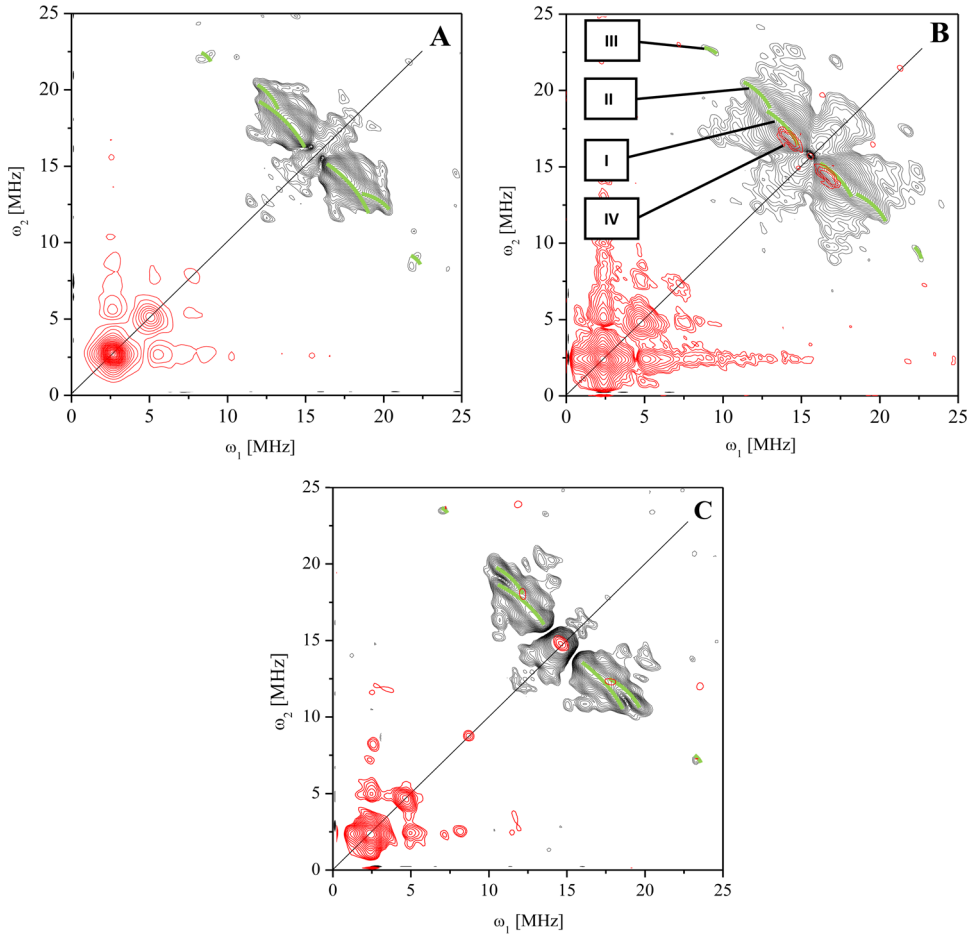

Figure 2. X-band HYSCORE spectra of reduced $HydF_{T.n.}$ before (black contour) and after (red contour) H/D exchange, recorded at field positions corresponding to the principal values of the g-tensor: (A) g_x, (B) g_y, and (C) g_z. Ridges corresponding to different proton sets are indicated. T = 10 K. Other acquisition parameters are reported in the Materials and Methods section.

contributions have been assumed due to the absence of precise structural data of the cluster and to the lack of spectroscopic constrains following the scarce orientation dependence of the spectrum. In this approximation, ridge I results in being characterized by a null isotropic hyperfine constant and a relatively small dipolar term T = 3.0 ± 0.5 MHz, in agreement with previously published results.[37] This dipolar term corresponds to a 3.0 ± 0.5 Å distance from the iron edge of the cluster, as calculated in the point dipole approximation.[51] The large uncertainty in the evaluated distance is determined by the error on the estimation of the dipolar interaction resulting from the assumptions and from the ambiguity on the projection factor (ranging from −0.70 to 1.83) of the total spin of the cluster onto the interacting iron ion, as described elsewhere.[52]

The simulation of ridge II requires a 3.5 ± 1 MHz isotropic hyperfine contribution and a 5 ± 1.0 MHz dipolar term, corresponding to a stronger interaction with the metal center and an estimated distance, based on the dipolar interaction, ranging from 2.1 to 3.0 Å. Although the simulation is affected by uncertainty due to the assumptions (axial tensor of the proton dipolar hyperfine interaction and spherical averaging), the need for a relatively large isotropic interaction denotes a sizable extension of the cluster wavefunction into the proton(s) of ridge II, thus supporting the hypothesis of a close proximity to the paramagnetic center.

According to the assignment to exchangeable protons, the hyperfine values used for the simulation of ridges I and II, scaled for the γ_H/γ_D factor, correctly simulate the signals appearing in the deuterium region, as reported in Figure 3. HYSCORE simulation has been performed also to reproduce the signals due to the set of nonexchangeable protons emerging in the proton region after the H/D exchange (protons IV in Table 2; calculated spectra are reported in the Supporting Information). The absence of isotropic hyperfine interaction and the small (2.5 ± 0.5 MHz) dipolar term, corresponding to a 3.3 ± 0.5 Å distance in the point dipole approximation, support the assignment to a set of protons belonging to protein residues surrounding the cluster. This is compatible with the environment of the cysteines of the conserved consensus sequence, as revealed by the analysis of the crystal structure of apo-$HydF_{T.n.}$, although a local conformational rearrangement of the protein scaffold is expected in the presence of the metal cluster.

In order to validate the hyperfine parameters obtained from HYSCORE simulations and determine the number of protons contributing to each ridge, which is not simply achievable by HYSCORE spectra simulation, 3p-ESEEM experiments on H/D-exchanged $HydF_{T.n.}$ have also been performed. The time traces and the frequency domain spectra obtained by Fourier transformation, collected in correspondence of six different values of the external magnetic field, ranging from g_z = 2.044 to g_x = 1.850, are shown in the Supporting Information. The 3p-

DOI: 10.1021/acs.jpcb.5b03110
J. Phys. Chem. B 2015, 119, 13680−13689

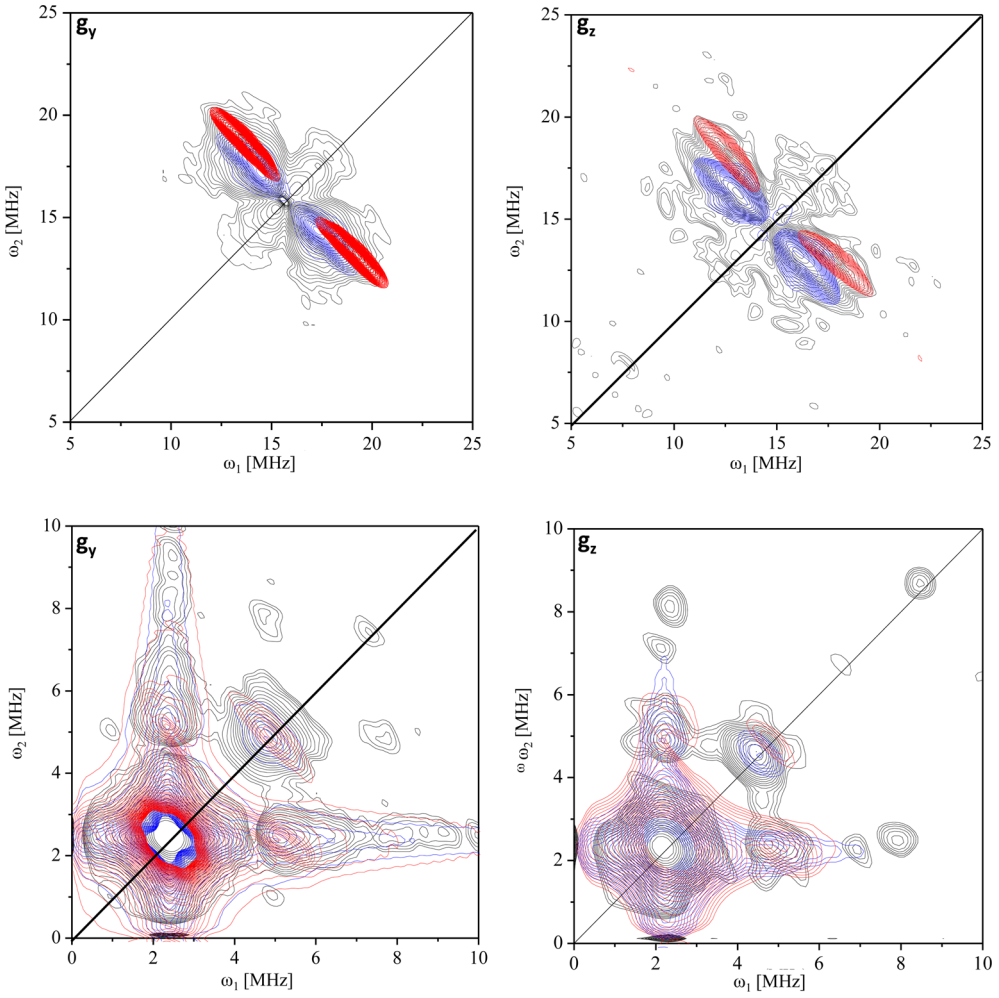

Figure 3. X-band HYSCORE spectra of the chemically reduced $HydF_{T.n.}$ measured at the two magnetic fields corresponding to g_y (1.90) and g_z (2.05). Experimental (black) and calculated spectra of exchangeable protons I (blue) and protons II (red). Top panels: proton region. Bottom panels: deuterium region.

Table 2. Hyperfine Coupling Parameters, Expressed As Isotropic (a_{iso}) and Dipolar (T) Contributions and the Corresponding Number of Protons Derived from the Simulation of HYSCORE and 3p-ESEEM Data of $HydF_{T.n.}$ along with the Estimated Distances of Protons to the [4Fe4S] Cluster, Calculated Using the Point Dipole Approximation

H	a_{iso} (MHz)	T (MHz)	distance (Å)	no. of nuclei (ESEEM)
I	0	3 ± 0.5	2.5−3.5	2
II	3.5 ± 1	5 ± 0.5	2.1−3.0	1
IV	0	2.5 ± 0.5	2.8−3.8	n.d.
V	0	0.035−0.125	5.2−10.4	30

ESEEM traces reveal the presence of deep modulations due to the interaction of the paramagnetic metal cluster with the surrounding deuterium nuclei. No orientation selection has emerged from the analysis of 3p-ESEEM traces, in agreement with the HYSCORE results. Simulations of the 3p-ESEEM time and frequency quotient traces, obtained after dividing the traces of deuterated samples by the corresponding ones of the protonated samples, have been performed using the same hyperfine parameters obtained from the HYSCORE analysis for the two exchangeable proton sets (ridges I and II). Results for the g_y field position are reported in Figure 4. Due to the absence of orientation selection in HYSCORE and ESEEM spectra, good fit has been achieved in the spherical limit, considering all of the orientations of the hyperfine tensor with respect to the g axes of the [4Fe−4S] cluster. Two deuterons for set I and a single deuteron belonging to set II, with the same parameters derived from the HYSCORE spectra, have been considered for the simulation. A set of 30 weakly interacting matrix deuterons (T = 0.035 ÷ 0.125 MHz) was also added to reproduce the experimental traces (protons V in Table 2). This latter contribution may be due to exchangeable protons belonging to the protein or to the water solvent molecules, approaching the cluster at a distance 5.2 < r < 10.4 Å, as calculated from the point dipole approximation.

DISCUSSION

Previously reported results on HydF proteins from different microorganisms have shown that only three conserved cysteines are strictly required for the binding of the [4Fe−4S] cluster, whereas the fourth ligand of the coordination sphere can vary depending on the molecular environment, as determined by local residues, and/or on the experimental conditions.[28] In the experiments carried out in both *T. neapolitana* and *T. maritima*, a [4Fe−4S] cluster−imidazole complex was detected in the presence of an excess of imidazole,

DOI: 10.1021/acs.jpcb.5b03110
J. Phys. Chem. B 2015, 119, 13680−13689

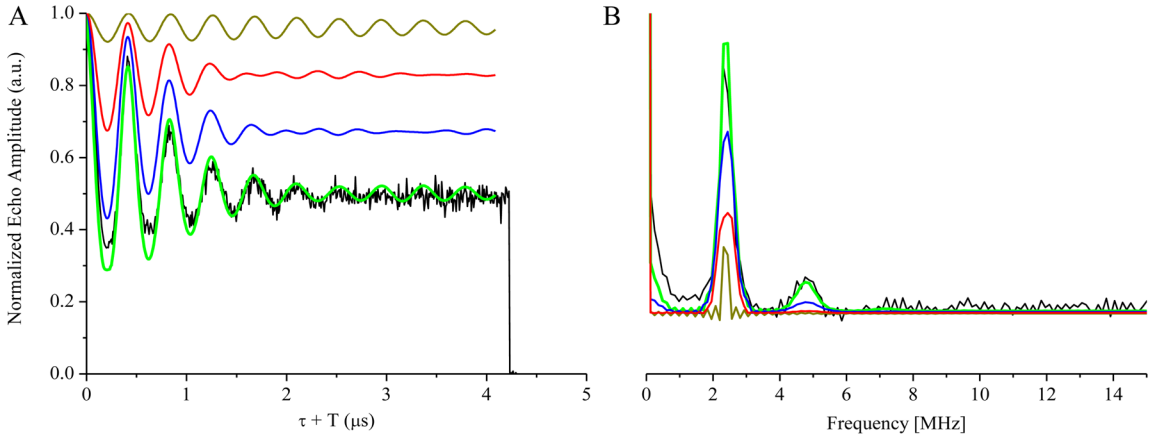

Figure 4. X-band 3p-ESEEM quotient traces of $HydF_{T.n.}$ H/D exchange recorded at a magnetic field corresponding to g = 1.90 (black), before (A) and after (B) Fourier transform; T = 10 K. Simulation as derived from the contributions of matrix protons (dark yellow), protons I (blue), and protons II (red) is reported as an orange bold line.

suggesting that the fourth metal coordination site is easily exchangeable. This may have important implications for the synthesis of the H-cluster precursor as an accessible iron coordination site could be relevant in binding and transfer of large substrates, such as the H-cluster precursor. Noncysteinyl ligation to cubane-type FeS clusters is known to occur in other enzymes, and in each case, the anomalous cluster coordination has a functional significance.[32] A small molecule from the buffer can make the fourth iron labile, explaining why these enzymes are often found to contain $[3Fe-4S]^{+}$ clusters in as-isolated or air-exposed conditions.[28]

Starting from these observations, we have performed H/D exchange experiments combined to advanced EPR methodologies to get insight into the proton environment of the metal cluster. On the basis of the results derived from the HYSCORE and 3p-ESEEM experiments, a new description of the proton environment of the [4Fe−4S] cluster of HydF is emerging. Two distinct sets of interacting protons, found in close proximity to the cluster (protons I and II), have been identified. They are both characterized by an easy exchangeability. The small number of these interacting exchangeable protons (I and II) is in agreement with the sharpness of the HYSCORE ridges. The poor orientation selection effects in the spectra reflect a not well-defined local structure for these protons. This is surprising in particular for proton II, the closest to the cluster with a Fe−H estimated distance of 2.1−3.0 Å, compatible with the values observed in other proteins for protons belonging to the coordinating ligands,[53−56] which is expected to be constrained in its possible orientations. However, it is possible that the higher spectral contribution, in terms of the number of nuclei, of the protons belonging to ridge I obscures the orientation dependence of the hyperfine interaction of the unique proton belonging to set II in the HYSCORE spectra. The presence of a sizable isotropic component of the hyperfine interaction characterizing this proton indicates a significant extension of the cluster wavefunction on it, revealing its proximity to the fourth ligand. Thus, excluding any coordination by proximal amino acidic residues, as proven by previous studies,[37] the experimental results of this work support the hypothesis that the fourth ligand is a protonated exogenous molecule. In this respect, it is worth noting that other examples have been reported in the literature for this type of coordination of the iron in Fe−S clusters. For instance, an organic sulfide has been observed as a ligand in the case of the [2Fe−2S] cluster of glutaredoxins,[57−63] while an hydroxyl ion is known to coordinate the [4Fe−4S] cluster of aconitase as well as those present in dihydroxy acid dehydratase enzymes.[43,64−66] There is a water molecule (or, in principle, a hydroxide ion) bound to the [4Fe−4S] cluster also in IspH,[67] with an Fe−O bond length of 2.1 Å. As a conclusion, on the basis of the spectroscopic results pointing to the presence of a interacting proton close to the cluster, we suggest that a similar hydroxyl ligation occurs also in HydF, although other singly protonated species cannot be excluded.

Protons belonging to set I are characterized by a smaller dipolar interaction, which corresponds to a longer Fe−H distance, and by local disorder. Many residues in close proximity to the cluster possess relatively acidic protons particularly prone to deuterium exchange. Because site-directed mutagenesis of putative coordinating residues E300, D310, D337, and Y380 left ridge I unaffected,[37] it is likely that the two protons of ridge I belong to an extra water molecule accessing the channel. The latter possibility is in agreement with the experimental evidence that imidazole, which is a larger molecule, is able to penetrate into the region surrounding the cluster, acting as a fourth ligand. Thus, it is reasonable to suppose that solvent molecules may as well approach the cluster site. This assignment of proton I to a water molecule would also explain the lack of orientation selection in the spectral features of the associated HYSCORE and ESEEM spectra because it is likely that it may assume different orientations depending on the dynamic H-bonding network determined not only by the protein environment but also by other, more distant solvent molecules present in the cavity. In facts, several matrix exchangeable protons are also needed in the simulation of the 3p-ESEEM traces, corresponding either to solvent molecules located at larger distance from the cluster or to distant protein exchangeable protons.

■ CONCLUSIONS

The H/D exchange experiments allow us to get new information on the description of the [4Fe−4S] cluster site of the maturase protein HydF from *T. neapolitana*. As has been noted, the presence of noncysteinyl ligands can strongly influence the physical properties of the FeS clusters, including stability and reactivity (for a recent review, see ref 68). However, only in a few cases reported in the literature has the

DOI: 10.1021/acs.jpcb.5b03110
J. Phys. Chem. B 2015, 119, 13680−13689

fourth ligand been fully assigned to a specific noncysteine protein residue. Binding of a substrate or a cofactor to the open coordination site of a [4Fe−4S] cluster, which in the absence of the substrate is occupied by a water molecule or hydroxide, has also been observed before, and in these cases, upon substrate binding, the water ligand is replaced by the substrate. Additionally, water molecules in the substrate binding pocket are also displaced.

HydF is known to be a maturation protein of the H-cluster, but the exact mechanism of the chemical reaction occurring at its active site is unknown. However, it may be speculated that because the initial step of the precursor assembly of the H-cluster occurs in HydG, it is likely that the synthon(s) is(are) passed to HydF successively. The results obtained in the present study showing the presence of an unusual ligation of the fourth iron atom of the [4Fe4−S] cluster, likely a hydroxyl ion, together with the presence of water molecules close to the metal center, which could be easily displaced by the entering precursor, points toward a high accessibility of the active site. This is in agreement with the need to harbor a large preformed H-cluster precursor. Subsequent transfer to the target apoprotein HydA should involve dissociation from the [4Fe−4S] cluster and rebinding of the exogenous ligand. This step may be mediated by the GTP-ase activity of HydF.

■ ASSOCIATED CONTENT

Supporting Information

Additional figures on HYSCORE and ESEEM of H/D-exchanged HydF. (1) Proton region of the HYSCORE spectrum of $HydF_{T.n.}$ after H/D exchange showing ridge IV; (2) 3p-ESEEM quotient traces of $HydF_{T.n.}$ after H/D exchange, recorded at different magnetic fields. The Supporting Information is available free of charge on the ACS Publications website at DOI: 10.1021/acs.jpcb.5b03110.

■ AUTHOR INFORMATION

Corresponding Authors

*E-mail: donatella.carbonera@unipd.it (D.C.).
*E-mail: paola.costantini@unipd.it (P.C.).

Notes

The authors declare no competing financial interest.

■ ACKNOWLEDGMENTS

This work has been supported by the CARIPARO Foundation (M3PC Project) by the MIUR (PRIN2010-2011 Prot. 2010FM38P_004).

■ REFERENCES

(1) Beinert, H.; Holm, R. H.; Münck, E. Iron−Sulfur Clusters: Nature's Modular, Multipurpose Structures. *Science* **1997**, *277*, 653−659.

(2) Lill, R. Function and Biogenesis of Iron−Sulphur Proteins. *Nature* **2009**, *460*, 831−838.

(3) Meyer, J. Iron−Sulfur Protein Folds, Iron−Sulfur Chemistry, and Evolution. *J. Biol. Inorg. Chem.* **2008**, *13*, 157−170.

(4) Fontecilla-Camps, J. C.; Amara, P.; Cavazza, C.; Nicolet, Y.; Volbeda, A. Structure−Function Relationships of Anaerobic Gas-Processing Metalloenzymes. *Nature* **2009**, *460*, 814−822.

(5) Vignais, P. M.; Billoud, B. Occurrence, Classification, and Biological Function of Hydrogenases: An Overview. *Chem. Rev.* **2007**, *107*, 4206−4272.

(6) Nicolet, Y.; Lemon, B. J.; Fontecilla-Camps, J. C.; Peters, J. W. A Novel FeS Cluster in Fe-Only Hydrogenases. *Trends Biochem. Sci.* **2000**, *25*, 138−143.

(7) Nicolet, Y.; de Lacey, A. L.; Vernede, X.; Fernandez, V. M.; Hatchikian, E. C.; Fontecilla-Camps, J. C. Crystallographic and FTIR Spectroscopic Evidence of Changes in Fe Coordination upon Reduction of the Active Site of the Fe-Only Hydrogenase from *Desulfovibrio desulfuricans*. *J. Am. Chem. Soc.* **2001**, *123*, 1596−1601.

(8) Silakov, A.; Wenk, B.; Reijerse, E.; Lubitz, W. ^{14}N HYSCORE Investigation of the H-Cluster of [FeFe] Hydrogenase: Evidence for a Nitrogen in the Dithiol Bridge. *Phys. Chem. Chem. Phys.* **2009**, *11*, 6592−6599.

(9) Posewitz, M. C.; King, P. W.; Smolinski, S. L.; Zhang, L.; Seibert, M.; Ghirardi, M. L. Discovery of Two Novel Radical *S*-Adenosylmethionine Proteins Required for the Assembly of an Active [Fe] Hydrogenase. *J. Biol. Chem.* **2004**, *279*, 25711−25720.

(10) Peters, J. W.; Broderick, J. B. Emerging Paradigms for Complex Iron−Sulfur Cofactor Assembly and Insertion. *Annu. Rev. Biochem.* **2012**, *81*, 429−450.

(11) Mulder, D. W.; Ortillo, D. O.; Gardenghi, D. J.; Naumov, A. V.; Ruebush, S. S.; Szilagyi, R. K.; Huynh, B.; Broderick, J. B.; Peters, J. W. Activation of $HydA^{\Delta EFG}$ Requires a Preformed [4Fe−4S] Cluster. *Biochemistry* **2009**, *48*, 6240−6248.

(12) Czech, I.; Silakov, A.; Lubitz, W.; Happe, T. The FeFe−Hydrogenase Maturase HydF from *Clostridium acetobutylicum* Contains a CO and CN-Ligated Iron Cofactor. *FEBS Lett.* **2010**, *584*, 638−642.

(13) Driesener, R. C.; Challand, M. R.; McGlynn, S. E.; Shepard, E. M.; Boyd, E. S.; Broderick, J. B.; Peters, J. W.; Roach, P. L. [FeFe]-Hydrogenase Cyanide Ligands Derived from *S*-Adenosylmethionine-Dependent Cleavage of Tyrosine. *Angew. Chem., Int. Ed.* **2010**, *49*, 1687−1690.

(14) McGlynn, S. E.; Shepard, E. M.; Winslow, M. A.; Naumov, A. V.; Duschene, K. S.; Posewitz, M. C.; Broderick, W. E.; Broderick, J. B.; Peters, J. W. HydF as a Scaffold Protein in [FeFe] Hydrogenase H-Cluster Biosynthesis. *FEBS Lett.* **2008**, *582*, 2183−2187.

(15) Rubach, J. K.; Brazzolotto, X.; Gaillard, J.; Fontecave, M. Biochemical Characterization of the HydE and HydG Iron-Only Hydrogenase Maturation Enzymes from *Thermotoga maritima*. *FEBS Lett.* **2005**, *579*, 5055−5060.

(16) Shepard, E. M.; McGlynn, S. E.; Bueling, A. L.; Grady-Smith, C. S.; George, S. J.; Winslow, M. a.; Cramer, S. P.; Peters, J. W.; Broderick, J. B. Synthesis of the 2Fe Subcluster of the [FeFe]-Hydrogenase H Cluster on the HydF Scaffold. *Proc. Natl. Acad. Sci. U.S.A.* **2010**, *107*, 10448−10453.

(17) Vallese, F.; Berto, P.; Ruzzene, M.; Cendron, L.; Sarno, S.; De Rosa, E.; Giacometti, G. M.; Costantini, P. Biochemical Analysis of the Interactions between the Proteins Involved in the FeFe-Hydrogenase Maturation Process. *J. Biol. Chem.* **2012**, *287*, 36544−36555.

(18) Berggren, G.; Adamska, A.; Lambertz, C.; Simmons, T. R.; Esselborn, J.; Atta, M.; Gambarelli, S.; Mouesca, J. M.; Reijerse, E.; Lubitz, W.; et al. Biomimetic Assembly and Activation of FeFe-Hydrogenases. *Nature* **2013**, *499*, 66−69.

(19) Esselborn, J.; Lambertz, C.; Adamska-Venkatesh, A.; Simmons, T.; Berggren, G.; Nothl, J.; Siebel, J.; Hemschemeier, A.; Artero, V.; Reijerse, E.; et al. Spontaneous activation of FeFe-Hydrogenases by an Inorganic 2Fe Active Site Mimic. *Nat. Chem. Biol.* **2013**, *9*, 607−609.

(20) Dinis, P.; Suess, D. L.; Fox, S. J.; Harmer, J. E.; Driesener, R. C.; De La Paz, L.; Swartz, J. R.; Essex, J. W.; Britt, R. D.; Roach, P. L. X-ray Crystallographic and EPR Spectroscopic Analysis of HydG, a Maturase in [FeFe]-Hydrogenase H-Cluster Assembly. *Proc. Natl. Acad. Sci. U.S.A.* **2015**, 1362−1367.

(21) Kuchenreuther, J. M.; Myers, W. K.; Suess, D. L.; Stich, T. A.; Pelmenschikov, V.; Shiigi, S. A.; Cramer, S. P.; Swartz, J. R.; Britt, R. D.; George, S. J. The HydG Enzyme Generates an $Fe(CO)_2(CN)$ Synthon in Assembly of the FeFe Hydrogenase H-Cluster. *Science* **2014**, *343*, 424−427.

(22) King, P. W.; Posewitz, M. C.; Ghirardi, M. L.; Seibert, M. Functional Studies of [FeFe] Hydrogenase Maturation in an *Escherichia coli* Biosynthetic System. *J. Bacteriol.* **2006**, *188*, 2163−2172.

DOI: 10.1021/acs.jpcb.5b03110
J. Phys. Chem. B 2015, 119, 13680−13689

(23) Czech, I.; Stripp, S.; Sanganas, O.; Leidel, N.; Happe, T.; Haumann, M. The FeFe-Hydrogenase Maturation Protein HydF Contains a H-Cluster Like 4Fe4S-2Fe Site. *FEBS Lett.* **2011**, *585*, 225−230.
(24) Dikanov, S. A.; Xun, L.; Karpiel, A. B.; Tyryshkin, A. M.; Bowman, M. K. Orientationally-Selected Two-Dimensional ESEEM Spectroscopy of the Rieske-Type Iron-Sulfur Cluster in 2,4,5-Trichlorophenoxyacetate Monooxygenase from *Burkholderia cepacia* AC1100. *J. Am. Chem. Soc.* **1996**, *118*, 8408−8416.
(25) Betz, J. N.; Boswell, N. W.; Fugate, C. J.; Holliday, G. L.; Akiva, E.; Scott, A. G.; Babbitt, P. C.; Peters, J. W.; Shepard, E. M.; Broderick, J. B. [FeFe]-Hydrogenase Maturation: Insights into the Role HydE Plays in Dithiomethylamine Biosynthesis. *Biochemistry* **2015**, *54*, 1807−1818.
(26) Brazzolotto, X.; Rubach, J. K.; Gaillard, J.; Gambarelli, S.; Atta, M.; Fontecave, M. The [Fe-Fe]-Hydrogenase Maturation Protein HydF from *Thermotoga maritima* is a GTPase with an Iron−Sulfur Cluster. *J. Biol. Chem.* **2006**, *281*, 769−774.
(27) Cendron, L.; Berto, P.; D'Adamo, S.; Vallese, F.; Govoni, C.; Posewitz, M. C.; Giacometti, G. M.; Costantini, P.; Zanotti, G. Crystal Structure of HydF Scaffold Protein Provides Insights into [FeFe]-Hydrogenase Maturation. *J. Biol. Chem.* **2011**, *286*, 1−12.
(28) Berto, P.; Di Valentin, M.; Cendron, L.; Vallese, F.; Albertini, M.; Salvadori, E.; Giacometti, G. M.; Carbonera, D.; Costantini, P. The [4Fe−4S]-Cluster Coordination of [FeFe]-Hydrogenase Maturation Protein HydF as Revealed by EPR and HYSCORE Spectroscopies. *Biochim. Biophys. Acta* **2012**, *1817*, 2149−2157.
(29) Berggren, G.; Garcia-Serres, R.; Brazzolotto, X.; Clemancey, M.; Gambarelli, S.; Atta, M.; Latour, J.-M.; Hernández, H. L.; Subramanian, S.; Johnson, M. K. An EPR/HYSCORE, Mössbauer, and Resonance Raman Study of the Hydrogenase Maturation Enzyme HydF: A Model for N-Coordination to [4Fe−4S] Clusters. *J. Biol. Inorg. Chem.* **2014**, *19*, 75−84.
(30) Moulis, J.-M.; Davasse, V. r.; Golinelli, M.-P.; Meyer, J.; Quinkal, I. The Coordination Sphere of Iron−Sulfur Clusters: Lessons from Site-Directed Mutagenesis Experiments. *J. Biol. Inorg. Chem.* **1996**, *1*, 2−14.
(31) Venkateswara Rao, P.; Holm, R. Synthetic Analogues of the Active Sites of Iron−Sulfur Proteins. *Chem. Rev.* **2004**, *104*, 527−560.
(32) Jiang, F.; McCracken, J.; Peisach, J. Nuclear Quadrupole Interactions in Cu(II)-Diethylenetriamine-Substituted. *J. Am. Chem. Soc.* **1990**, *112*, 9035−9044.
(33) Hinckley, G. T.; Frey, P. A. Cofactor Dependence of Reduction Potentials for 4Fe−4S (2+/1+) in Lysine 2,3-Aminomutase. *Biochemistry* **2006**, *45*, 3219−3225.
(34) Broderick, J. B.; Duffus, B. R.; Duschene, K. S.; Shepard, E. M. Radical *S*-Adenosylmethionine Enzymes. *Chem. Rev.* **2014**, *114*, 4229−4317.
(35) Holm, R. H.; Kennepohl, P.; Solomon, E. I. Structural and Functional Aspects of Metal Sites in Biology. *Chem. Rev.* **1996**, *96*, 2239−2314.
(36) Lubitz, W.; Ogata, H.; RuL diger, O.; Reijerse, E. Hydrogenases. *Chem. Rev.* **2014**, *114*, 4081−4148.
(37) Albertini, M.; Vallese, F.; Di Valentin, M.; Berto, P.; Giacometti, G. M.; Costantini, P.; Carbonera, D. The Proton Iron−Sulfur Cluster Environment of the [FeFe]-Hydrogenase Maturation Protein HydF from *Thermotoga neapolitana*. *Int. J. Hydrogen Energy* **2014**, *39*, 18574−18582.
(38) Stoll, S.; Schweiger, A. EasySpin, a Comprehensive Software Package for Spectral Simulation and Analysis in EPR. *J. Magn. Reson.* **2006**, *178*, 42−55.
(39) Mims, W. B.; Davis, J. L.; Peisach, J. The Accessibility of Type I Cu(II) Centers in Laccase, Azurin, and Stellacyanin to Exchangeable Hydrogen and Ambient Water. *Biophys. J.* **1984**, *45*, 755−766.
(40) Mims, W. Elimination of the Dead-Time Artifact in Electron Spin−Echo Envelope Spectra. *J. Magn. Reson.* **1984**, *59*, 291−306.
(41) Edmonds, D.; Goren, S.; Mackay, A.; White, A.; Sherman, W. The Nuclear Quadrupole Resonance of 2D and ^{17}O in Ice II. *J. Magn. Reson.* **1976**, *23*, 505−514.
(42) Stoll, S.; Britt, R. D. General and Efficient Simulation of Pulse EPR Spectra. *Phys. Chem. Chem. Phys.* **2009**, *11*, 6614−6625.
(43) Werst, M. M.; Kennedy, M. C.; Beinert, H.; Hoffman, B. M. ^{17}O, ^{1}H, and ^{2}H Electron Nuclear Double Resonance Characterization of Solvent, Substrate, and Inhibitor Binding to the Iron−Sulfur [4Fe−4S]$^{+}$ Cluster of Aconitase. *Biochemistry* **1990**, *29*, 10526−10532.
(44) Antonkine, M. L.; Koay, M. S.; Epel, B.; Breitenstein, C.; Gopta, O.; Gärtner, W.; Bill, E.; Lubitz, W. Synthesis and Characterization of de novo Designed Peptides Modelling the Binding Sites of [4Fe−4S] Clusters in Photosystem I. *Biochim. Biophys. Acta* **2009**, *1787*, 995−1008.
(45) Kappl, R.; Ebelsh, M.; H, F. Probing Electronic and Structural Properties of the Reduced [2Fe−2S] Cluster by Orientation-Selective ^{1}H ENDOR Spectroscopy: Adrenodoxin versus Rieske Iron−Sulfur Protein. *Appl. Magn. Reson.* **2006**, *459*, 427−459.
(46) Foerster, S.; van Gastel, M.; Brecht, M.; Lubitz, W. An Orientation-Selected ENDOR and HYSCORE Study of the Ni−C Active State of *Desulfovibrio vulgaris* Miyazaki F Hydrogenase. *J. Biol. Inorg. Chem.* **2005**, *10*, 51−62.
(47) Canne, C.; Ebelshauser, M.; Gay, E.; Shergill, J. K.; Cammack, R.; Kappl, R. Hc Probing Magnetic Properties of the Reduced [2Fe−2S] Cluster of the Ferredoxin from *Arthrospira platensis* by ^{1}H ENDOR Spectroscopy. *J. Biol. Inorg. Chem.* **2000**, *5*, 514−526.
(48) Kappl, R.; Ciurli, S.; Luchinat, C. Probing Structural and Electronic Properties of the Oxidized $[Fe_4S_4]^{3+}$ Cluster of *Ectothiorhodospira halophila* iso-II High-Potential Iron−Sulfur Protein by ENDOR Spectroscopy. *J. Am. Chem. Soc.* **1999**, *121*, 1925−1935.
(49) Dean, P. E.; Fan, C.; Hoffman, B. M. Pulsed Proton−Deuterium $^{1,2}H$ ENDOR and $^{2}H-^{2}H$ TRIPLE Resonance of H-Bonds and Cysteinyl β-CH_2 of the *D. gigas* Hydrogenase [3Fe−4S]$^{(+)}$ Cluster. *J. Am. Chem. Soc.* **1994**, *116*, 1033−1041.
(50) Poppl, A.; Kevan, L. A Practical Strategy for Determination of Proton Hyperfine Interaction Parameters in Paramagnetic Transition Metal Ion Complexes by Two-Dimensional HYSCORE Electron Spin Resonance Spectroscopy in Disordered Systems. *J. Phys. Chem.* **1996**, *100*, 3387−3394.
(51) Schweiger, A.; Jeschke, G. *Principles of Pulse Electron Paramagnetic Resonance*; Oxford University Press: Oxford, U.K., 2001.
(52) Mouesca, J.-M.; Noodleman, L.; Case, D.; Lamotte, B. Spin Densities and Spin Coupling in Iron−Sulfur Clusters: A New Analysis of Hyperfine Coupling Constants. *Inorg. Chem.* **1995**, *34*, 4347−4359.
(53) Gloux, J.; Gloux, P.; Laugier, J. Single-Crystal and Powder EPR Studies of the $S = 1/2$ Ground State of the Iron−Sulfur Core in [Tris(tetraethylammonium)][tetrakis (benzylthiolato)tetrakis(μ_3-sulfido)-tetrairon]·(*N*,*N*-Dimethylformamide) with Crystal Structure Determination. *J. Am. Chem. Soc.* **1996**, *118*, 11644−11653.
(54) Lloyd, S.; Lauble, H.; Prasad, G.; Stout, C. The Mechanism of Aconitase: 1.8 A Resolution Crystal Structure of the S642A: Citrate Complex. *Protein Sci.* **1999**, *8*, 2655−2662.
(55) Nicolet, Y.; Piras, C.; Legrand, P.; Hatchikian, C. E.; Fontecilla-Camps, J. C. *Desulfovibrio desulfuricansiron* Hydrogenase: The Structure Shows Unusual Coordination to an Active Site Fe Binuclear Center. *Structure* **1999**, *7*, 13−23.
(56) Nielsen, M. S.; Harris, P.; Ooi, B. L.; Christensen, H. E. The 1.5 C Resolution Crystal Structure of $[Fe_3S_4]$-Ferredoxin from the Hyperthermophilic Archaeon *Pyrococcus furiosus*. *Biochemistry* **2004**, *43*, 5188−5194.
(57) Berndt, C.; Hudemann, C.; Hanschmann, E.-M.; Axelsson, R.; Holmgren, A.; Lillig, C. H. How Does Iron−Sulfur Cluster Coordination Regulate the Activity of Human Glutaredoxin 2. *Antioxid. Redox Signaling* **2007**, *9*, 151−157.
(58) Iwema, T.; Picciocchi, A.; Traore, D. A. K.; Ferrer, J. L.; Chauvat, F.; Jacquamet, L. Structural Basis for Delivery of the Intact Fe_2S_2 Cluster by Monothiol Glutaredoxin. *Biochemistry* **2009**, *48*, 6041−6043.
(59) Johansson, C.; Kavanagh, K. L.; Gileadi, O.; Oppermann, U. Reversible Sequestration of Active Site Cysteines in a 2Fe−2S-Bridged Dimer Provides a Mechanism for Glutaredoxin 2 Regulation in Human Mitochondria. *J. Biol. Chem.* **2007**, *282*, 3077−3082.

DOI: 10.1021/acs.jpcb.5b03110
J. Phys. Chem. B 2015, 119, 13680−13689

(60) Johansson, C.; Roos, A. K.; Montano, S. J.; Sengupta, R.; Filippakopoulos, P.; Guo, K.; von Delft, F.; Holmgrent, A.; Oppermann, U.; Kavanagh, K. L. The Crystal Structure of Human GLRX5: Iron−Sulfur Cluster Co-ordination, Tetrameric Assembly and Monomer Activity. *Biochem. J.* **2011**, *433*, 303−311.
(61) Li, H. R.; Mapolelo, D. T.; Dingra, N. N.; Naik, S. G.; Lees, N. S.; Hoffman, B. M.; Riggs-Gelasco, P. J.; Huynh, B. H.; Johnson, M. K.; Outten, C. E. The Yeast Iron Regulatory Proteins Grx3/4 and Fra2 Form Heterodimeric Complexes Containing a 2Fe−2S Cluster with Cysteinyl and Histidyl Ligation. *Biochemistry* **2009**, *48*, 9569−9581.
(62) Rouhier, N.; Unno, H.; Bandyopadhyay, S.; Masip, L.; Kim, S. K.; Hirasawa, M.; Gualberto, J. M.; Lattard, V.; Kusunoki, M.; Knaff, D. B.; et al. Functional, Structural, and Spectroscopic Characterization of a Glutathione-Ligated Fe−2S Cluster in Poplar Glutaredoxin C1. *Proc. Natl. Acad. Sci. U.S.A.* **2007**, *104*, 7379−7384.
(63) Hedderich, R.; Hamann, N.; Bennati, M. Heterodisulfide Reductase from Methanogenic Archaea: A New Catalytic Role for an Iron−Sulfur Cluster. *Biol.Chem.* **2005**, *386*, 961−970.
(64) Flint, D.; Emptage, M.; Finnegan, M.; Fu, W.; Johnson, M. The Role and Properties of the Iron−Sulfur Cluster in *Escherichia coli* Dihydroxy-Acid Dehydratase. *J. Biol. Chem.* **1993**, *268*, 14732−1474.
(65) Knauer, S. H.; Buckel, W.; Dobbek, H. Structural Basis for Reductive Radical Formation and Electron Recycling in (R)-2-Hydroxyisocaproyl-CoA Dehydratase. *J. Am. Chem. Soc.* **2011**, *133*, 4342−4347.
(66) Telser, J.; Emptage, M.; Merkle, H.; Kennedy, M. C.; Beinert, H.; Hoffman, B. M. ^{17}O Electron Nuclear Double Resonance Characterization of Substrate Binding to the $[4Fe-4S]^{1+}$ Cluster of Reduced Active Aconitase. *J. Biol. Chem.* **1986**, *261*, 4840−4846.
(67) Span, I.; Wang, K.; Wang, W.; Zhang, Y.; Bacher, A.; Eisenreich, W.; Li, K.; Schulz, C.; Oldfield, E.; Groll, M. Discovery of Acetylene Hydratase Activity of the Iron−Sulphur Protein IspH. *Nat. Commun.* **2012**, *3*, 1042.
(68) Bak, D. W.; Elliott, S. J. Alternative FeS Cluster Cigands: Tuning Redox Potentials and Chemistry. *Curr. Opin. Chem. Biol.* **2014**, *19*, 50−58.

DOI: 10.1021/acs.jpcb.5b03110
J. Phys. Chem. B 2015, 119, 13680−13689